ADVANCED FUNCTIONAL MATERIALS
www.afm-journal.de

Highly Fluorescent Nanodiamonds Protein-Functionalized for Cell Labeling and Targeting

Be-Ming Chang, Hsin-Hung Lin, Long-Jyun Su, Wen-Der Lin, Ruey-Jen Lin, Yan-Kai Tzeng, Reiko T. Lee, Yuan C. Lee, Alice L. Yu, and Huan-Cheng Chang**

Fluorescent nanodiamond (FND) is attracting much attention as a bioimaging agent because of its inherent biocompatibility and superior optical properties (e.g., excellent photostability and far-red emission). However, for practical use in life science research, some issues such as higher brightness and ease of bioconjugation have to be solved. Here, it is shown that the 100-nm FND particles fabricated by using nitrogen-rich type Ib diamonds and high-energy proton irradiation are highly fluorescent and readily functionalizable with proteins for biological applications. In the first approach, acid-treated FND is noncovalently coated with glycoproteins or neoglycoproteins (i.e., proteins chemically modified with multiple sugar residues) for targeting hepatocytes via carbohydrate receptors. In the second approach, FND is first PEGylated and then covalently conjugated with streptavidin, to which biotin-labeled antibodies of interest are linked. High targeting specificity of the bioconjugated FND is demonstrated with the human hepatoma cell line, HepG2, and breast cancer cell lines, ASB145-1R, MCF-7, and MDA-MB-231 cells. These approaches should be widely applicable to a variety of situations for specific targeting and labeling of cells.

1. Introduction

Synthetic nanoparticles are promising and versatile tools for biomedical imaging applications. A large number of experiments have demonstrated that the use of nanoparticles such as semiconductor quantum dots, nanogold, super-paramagnetic iron oxides, and carbon nanotubes can significantly improve image quality over conventional contrast agents.[1] Fluorescent nanodiamond (FND), containing a high density ensemble (≈10 ppm) of negatively charged nitrogen-vacancy centers as built-in fluorophores (emission wavelength of 600–800 nm), has recently emerged as an attractive alternative to molecular fluorophores such as organic dyes and fluorescent proteins for optical bioimaging. The sp^3-carbon-based nanomaterials have no problems associated with chemical degradation,[2] photobleaching,[3–5] exocytosis,[6,7] and toxicity.[2,3,8–10] When properly conjugated with bioactive ligands or grafted with high-specificity antibodies through biotin-avidin interactions,[11,12] they are useful as tools for targeted cell labeling and long-term cell imaging and tracking applications, both in vitro and in vivo.

To facilitate practical use of nanodiamonds in biology and nanoscale medicine,[13–17] considerable research efforts have been devoted to the development of new surface functionalization methods to enhance the bioconjugation ability of the nanomaterial.[18] However, only few studies are available on the specific labeling of cells with FND.[19–23] A major hurdle in this study is that nanoparticles (including FND) are prone to aggregation in physiological medium, such as phosphate-buffered saline (PBS),[24] resulting in nonspecific labeling. We have

B.-M. Chang, L.-J. Su, Y.-K. Tzeng, Prof. H.-C. Chang
Institute of Atomic and Molecular Sciences
Academia Sinica, Taipei 106, Taiwan
E-mail: hchang@gate.sinica.edu.tw
B.-M. Chang, Prof. H.-C. Chang
Taiwan International Graduate Program–Molecular Science and Technology
Academia Sinica, Taipei 115 Taiwan
B.-M. Chang
Department of Chemistry
National Tsing Hua University
Hsinchu 300, Taiwan
H.-H. Lin, W.-D. Lin, R.-J. Lin, Prof. A. L. Yu
Genomics Research Center
Academia Sinica, Taipei 115, Taiwan
E-mail: ayu@gate.sinica.edu.tw
Prof. A. L. Yu, H.-H. Lin
Taiwan International Graduate Program–Chemical Biology and Molecular Biophysics
Academia Sinica, Taipei 115, Taiwan
W.-D. Lin
Graduate Institute of Life Sciences
National Defense Medical Center
Taipei 114, Taiwan
Prof. Y. C. Lee, Dr. Reiko T. Lee
Biology Department
Johns Hopkins University
Baltimore, MD 21218, USA
Prof. A. L. Yu
Department of Pediatrics
University of California in San Diego, San Diego, CA 92103, USA

DOI: 10.1002/adfm.201301075

recently found that bovine serum albumin (BSA) is an excellent stabilizing agent and diamond nanoparticles coated with BSA can resist flocculation in PBS for more than a week.[25] The coating can be made simply by physical adsorption, rendering it practical to perform targeted cell labeling with bioconjugated FND. Here, we present methods to conjugate proteins either noncovalently or covalently with FND for ligand-based targeting and antibody-based labeling of mammalian cells. Additionally, we show that by performing ion irradiation with 3-MeV protons[26,27] and using nitrogen-rich type Ib diamond crystallites[28] as the starting material, it is possible to fabricate highly bright FND suitable for cell sorting applications. We illustrate the usage of these protein-conjugated FND particles with flow cytometry and confocal fluorescence microscopy.

In the first example of the application, FND was surface-functionalized by noncovalent coating of BSA chemically modified with carbohydrate ("neoglycoprotein") such as galactose (Gal), N-acetylgalactosamine (GalNAc), and lactose (Lac) for hepatic targeting. Liver is an important organ for homeostasis that produces many important biomolecules including acute-phase proteins.[29] Liver is also unique in that it is endowed with a powerful carbohydrate receptor, the asialoglycoprotein receptor (ASGPR), which is highly specific for Gal- and GalNAc-terminated glycans and is present in a large number on the mammalian hepatocyte surface (ca. 400 000 copies on the rat hepatocyte surfaces[30]). These mammalian ASGPRs, also known as Ashwell–Morell receptors (AMRs),[31] possess an amazing characteristic of dramatically responding to multivalency of target sugars and to their spatial arrangement (i.e., the glycoside clustering effect).[31–33] Taking advantage of this effect, we synthesized BSA modified with either 2 TriGalNAc or more than 20 lactose molecules,[34,35] and attached them to the surface of acid-treated FND for specific targeting of liver cancer cells. TriGalNAc is a synthetic compound that contains 3 terminal GalNAc residues exhibiting a high affinity (with a dissociation constant in the nM range) to ASGPR on hepatocytes.[35] We demonstrated the applicability of the neoglycoprotein-coated FND for hepatic targeting in vitro using the HepG2 cell line.[36,37]

The second example consists of FND conjugated with antibodies for specific labeling of CD44 and CD55 antigens on cell surfaces. The former is a glycoprotein widely expressed in mammalian cell types[38] and the latter is a glycoprotein broadly distributed among hematopoietic and non-hematopoietic cells.[39] Three human breast carcinoma cell lines were used in this study: MCF-7, ASB145-1R, and MDA-MB-231. The first two cell types express different levels of CD44, presenting an interesting case for comparison, whereas the last cell type expresses CD55 with a hemagglutinin (HA) tag, thus allowing for colocalization studies of anit-CD55 and anti-HA antibodies labeled with FND and organic dye, respectively, by fluorescence imaging. In this experiment, SA-PEG-FND was first prepared by PEGylation of FND,[20,40,41] followed by covalent conjugation of streptavidin (SA). Targeted labeling was then carried out by using the particles for high-affinity interaction with biotinylated antibodies that bind specifically with the extracellular epitopes of CD44 or CD55. Thanks to the excellent photostability of FND, the events before and after endocytosis of the particles in the individual cells could be tracked over an extended period of time by confocal fluorescence imaging.

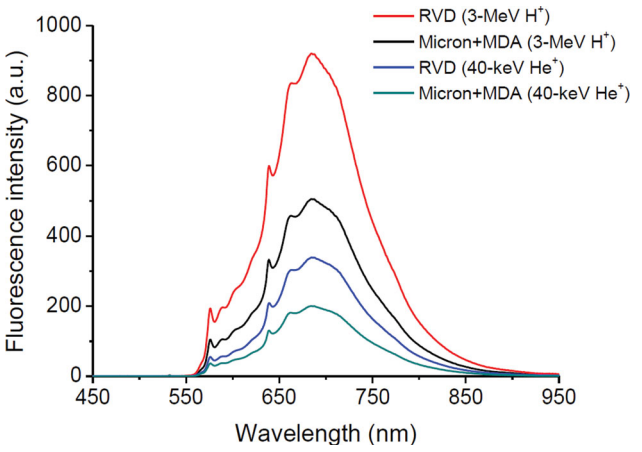

Figure 1. Dispersed fluorescence spectra of FND particles suspended in water. The FND samples (size of ≈100 nm) were prepared with two different starting materials (Micron+MDA and RVD) under two different ion irradiation conditions (40-keV He^+ and 3-MeV H^+). The spectra were obtained by exciting the particles (concentration of 1 mg mL^{-1}) at 532 nm and the fluorescence was analyzed with a multichannel spectrometer.

2. Result and Discussion

2.1. FND Characterization

FND was prepared by ion bombardment of monocrystalline diamond powders using either 40-keV He^+ or 3-MeV H^+ as damaging agents.[26,27] Two diamond materials were employed in this study, Micron+MDA and RVD, with a measured nitrogen density of ≈100 ppm and ≈200 ppm, respectively.[28] **Figure 1** compares the fluorescence spectra of four FND samples prepared with either Micron+MDA or RVD under two different ion irradiation conditions. For FND fabricated by using He^+ or H^+ irradiation, the N-richer diamond consistently showed an approximately twofold higher fluorescence intensity, which correlates well with the increased nitrogen density in the diamond matrix. The employment of this N-richer diamond, together with the treatment with 3-MeV protons, yielded FND with the highest fluorescence brightness we have achieved so far. Compared with the FND fabricated by using 40-keV He^+ irradiation of Micron+MDA diamond as typically used in our previous experiments,[7,9,10] the sample is fourfold higher in fluorescence intensity. As will be discussed in the following sections, this fourfold improvement is crucial for flow cytometric analysis of cells expressing different levels of CD44 with FND as a fluorescent marker.

2.2. Noncovalent Conjugation of FND with (neo)glycoproteins

Prior to bioconjugation, FND surfaces were first functionalized with carboxyl and other oxygen-containing groups (such as–OH,–C = O, and–C-O-C–) by strong oxidative acid treatment.[26] Dynamic light scattering (DLS) measurements indicated that the bare FND has a number-averaged diameter of ≈100 nm in deionized distilled water (DDW) (**Figure 2**a). The particles were then noncovalently coated with neoglycoproteins including TriGalNAc-BSA and Lac-BSA only (**Scheme 1**a) for ligand-based

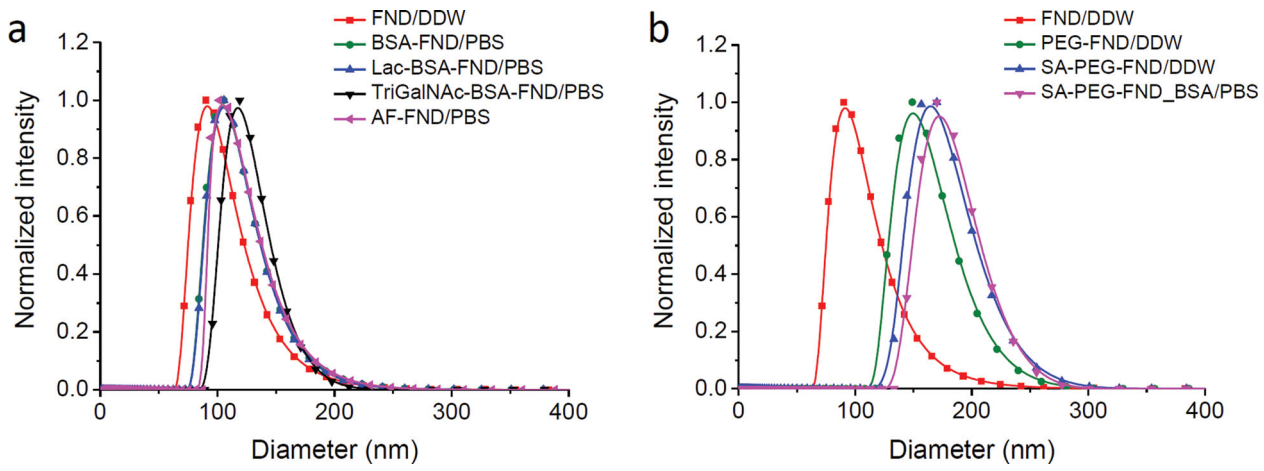

Figure 2. Size measurements of bare and protein-conjugated FND in DDW or PBS by dynamic light scattering. a) FND noncovalently coated with proteins at the weight (mg) to mole (nmol) ratios of FND:BSA = 1:5, FND:Lac-BSA = 1:5, FND:TriGalNAc-BSA = 1:10, and FND:AF = 1:10. b) FND covalently conjugated with PEG and then with SA at the weight ratio of FND:PEG:SA = 1:5:0.2, followed by noncovalent coating of the SA-PEG-FND conjugates with BSA to avoid particle aggregation in PBS.

targeting. The coating was made by physical adsorption through the interplay of electrostatic force, hydrogen bonding, and hydrophobic interactions between proteins and surfaces.[42,43] Asialofetuin (AF), a glycoprotein having three asparagine-connected triantennary complex sugar chains with terminal galactose residues,[44] was also used for comparison. As shown by DLS in Figure 2a, these nanoparticle bioconjugates could be stably dispersed in PBS when FND was properly coated with proteins at the weight (mg) to mole (nmol) ratios of FND:Lac-BSA = 1:5, FND:TriGalNAc-BSA = 1:10, and FND:AF = 1:10 in water. To verify the validity of the conjugation, Lac-BSA-FND was first stained by biotinylated Vicia villosa lectin, then by FITC-streptavidin, and finally imaged by confocal fluorescence microscopy on a glass slide (Supporting Information Figure S1a). The colocalization of the FND signal with that of the fluorescently labeled lectin confirmed that the neoglycoproteins have been successfully grafted on the FND surface. It should be noted that while the conjugation of the carboxylated/oxidized FND with the proteins is noncovalent, the binding between them is so strong that no significant desorption occurred during the course of the present study, as evidenced from the SDS-PAGE (sodium dodecyl sulfate polyacrylamide gel electrophoresis) analysis of FND conjugated with unmodified BSA for more than 5 h (see Supporting Information Figure S2 and ref. [42] for details).

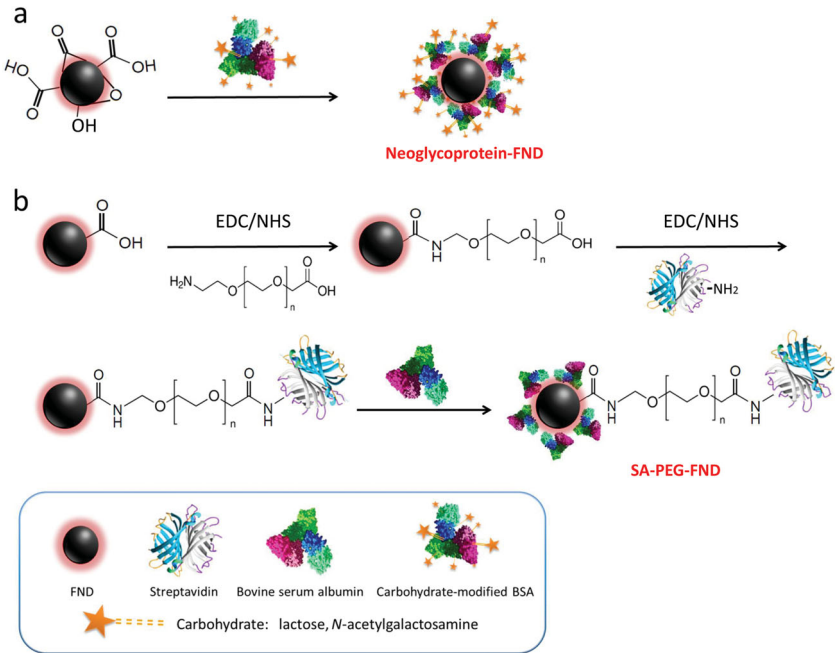

Scheme 1. Workflows of the bioconjugation of FND. a) Grafting of (neo)glycoproteins on FND. The proteins are attached to the surface of acid-washed FND by physical adsorption. b) Grafting of streptavidin on FND. The grafting starts with activation of the surface carboxyl groups on FND with EDC and NHS, forming amine-reactive terminus. The FND is then conjugated with carboxyl PEG amines via carboxyl-to-amine cross-linking. Further activation leads to covalent coupling between of the carboxyl groups of PEG-FND and the primary amine groups ($-NH_2$) of streptavidin through amide bond formation. Finally, the SA-conjugated PEG-FND is noncovalently covered with BSA to prevent particle aggregation in PBS.

2.3. Covalent Conjugation of FND with Streptavidin

A previous study has shown that the level of carboxyl groups on FND after harsh acid treatment is ≈7%,[45] which is sufficient for ensuing surface modification. To conduct antibody-based labeling, the–COOH groups of FND were first reacted with the amino group of NH_2-PEG-COOH. The–COOH of the PEG was then used

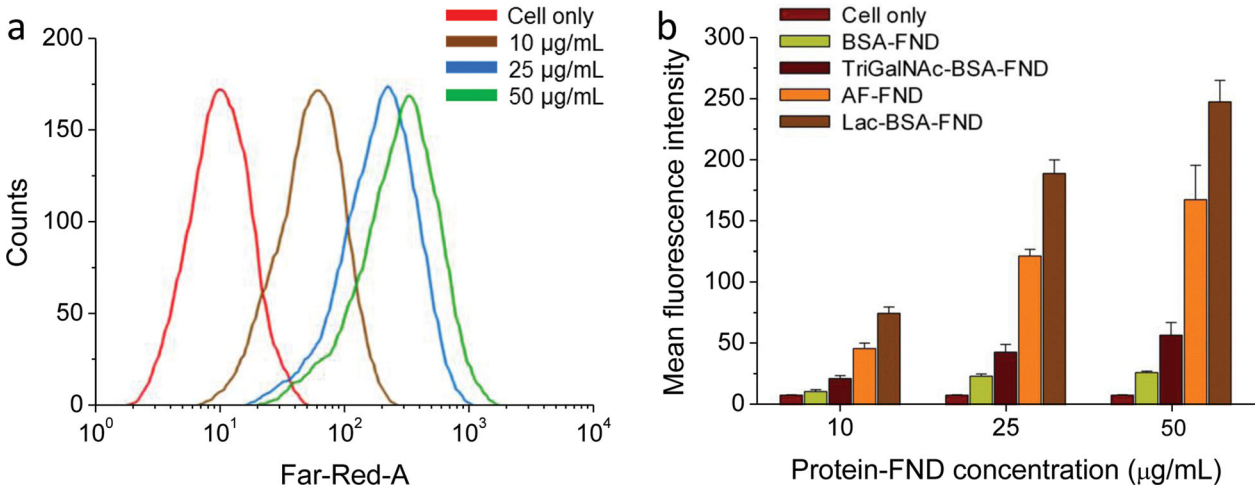

Figure 3. Flow cytometric analysis of the uptakes of protein-conjugated FND by HepG2 cells. a) A typical result for HepG2 cells labeled with Lac-BSA-FND at different concentrations (0, 10, 25, and 50 μg mL^{-1}). b) Mean fluorescence intensities as a function of the concentration of the labeling agent, as annotated in the figure, showing different levels of the uptake of BSA-, neoglycoprotein-, and glycoprotein-conjugated FND. The intensities were calculated based on the flow cytometry data, as displayed in panel (a) for Lac-BSA-FND and other protein-FND conjugates (data not shown). All the particles were incubated with the cells for 4 h to allow cellular uptake. Each experiment was repeated independently three times.

to conjugate with SA through amidation (Scheme 1b).[46] Any open sites on the FND surface were subsequently covered with unmodified BSA to avoid particle agglomeration as verified by particle size measurement (Figure 2b). The efficacy of the bioconjugation was further tested by fluorescence imaging of SA-PEG-FND stained with biotinylated DyLight488 on a glass slide. The colocalization of FND and DyLight488 fluorescence signals in Supporting Information Figure S1b confirmed that the conjugation between SA and FND is successful. It should be stressed that in these experiments, it is critically important to ensure good dispersibility of the SA-conjugated FND in high-salt media, since particle agglomeration and/or precipitation almost always lead to nonspecific labeling. Additionally, cells should be labeled in an inverted configuration (Supporting Information Figure S3)[25,47] to avoid undesirable precipitation or deposition of the nanoparticles on cell surfaces.

2.4. Ligand-Based Targeting

FND, prepared with Micron+MDA diamond and 40-keV He^+ irradiation, was grafted with Lac-BSA, TriGalNAc-BSA, or AF to target HepG2 cells by incubation at 37 °C for 4 h. As revealed by DLS (Figure 2a) and flow cytometric analysis (**Figure 3**a), the surface modification of FND not only prevents aggregation of the particles in PBS and cell culture media, but also endows them with good specific targeting ability for ASGPR on HepG2. Only particles coated with the neoglycoproteins or glycoproteins were substantially taken up by the cells. The amount of the particle uptake, which is proportional to the mean fluorescence intensity, increased steadily with the increasing concentration of the FND-bioconjugates from 10 to 50 μg mL^{-1} (Figure 3b). Confocal fluorescence imaging confirmed the presence of Lac-BSA-FND, TriGalNAc-BSA-FND, and AF-FND inside the HepG2 cells, but negligible for BSA-FND (**Figure 4**a–h), which lacks suitable ligands to target ASGPR. Compared with PEGylated quantum dots capped with galactosamine (GalN)[36] and iron oxide nanoparticles covalently conjugated with Gal,[37] our Lac-BSA-FND appears to show better performance according to the flow cytometric analysis. At the concentration of 50 μg mL^{-1}, the mean fluorescence intensity of the HepG2 cells with the Lac-BSA-FND labeling was ≈10-fold greater than that of the same cells labeled by BSA-FND. It can be compared to the corresponding ≈5-fold increase for cells labeled with 20 nmol GalN-capped quantum dots and also 100 μg mL^{-1} Gal-conjugated iron oxide nanoparticles.

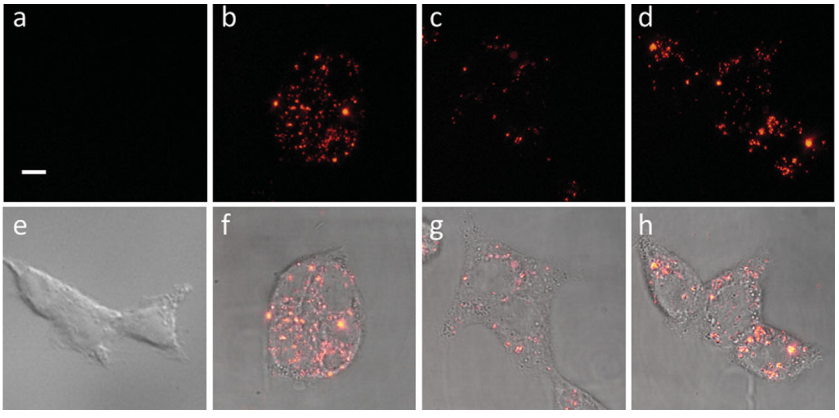

Figure 4. Bright-field and confocal fluorescence images of protein-conjugated FND internalized by HepG2 cells: a,e) BSA-FND, b,f) Lac-BSA-FND, c,g) TriGalNAc-BSA-FND, and d,h) AF-FND. Displayed in are a–d) Z-stacked confocal fluorescence images and e–h) are overlays of bright-field and confocal fluorescence images. Scale bar is 10 μm.

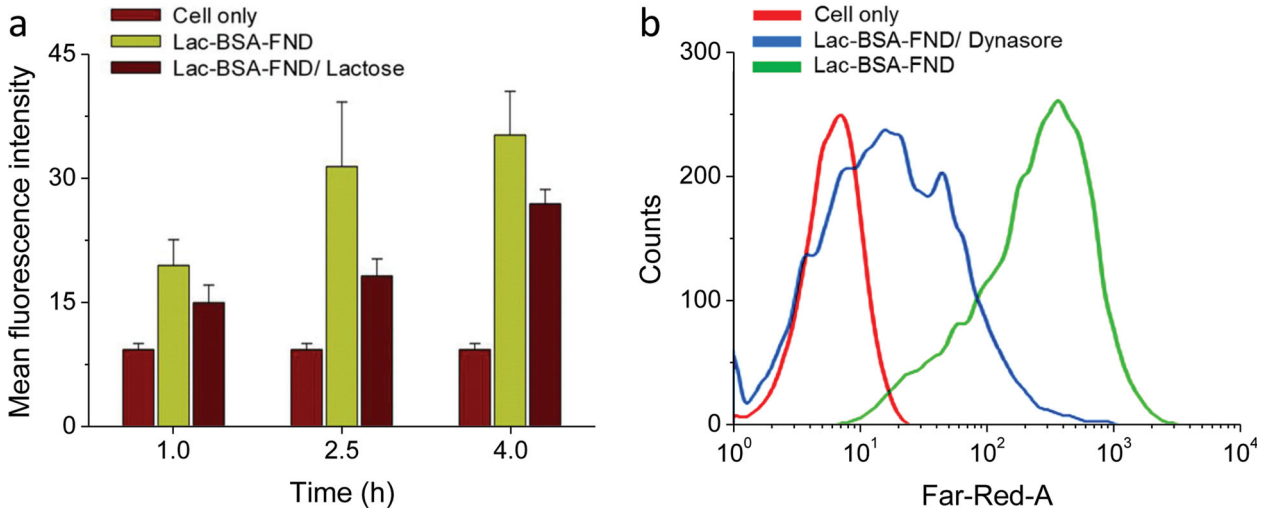

Figure 5. a) Competition and b) inhibition assays for the uptake of Lac-BSA-FND by HepG2 cells measured by flow cytometry. In (a), the cellular uptake of Lac-BSA-FND (50 μg mL^{-1}) was significantly suppressed due to the presence of lactose (0.3 M), showing the competition for binding with ASGPR by free lactose. Each experiment was repeated independently three times. In (b), the uptake of Lac-BSA-FND was markedly reduced after pre-incubation with dynasore (0.24 mM), which is indicative of receptor-mediated endocytosis.

The HepG2 targeting efficacy was also examined with a competition assay using free ligands to inhibit their binding with ASGPR.[37] As shown in **Figure 5**a, the uptake of Lac-BSA-FND by HepG2 cells was significantly suppressed in the presence of free lactose (0.3 M) at various incubation time points (1–4 h). The FND uptake mechanism was further studied by using endocytosis inhibitors. In this assay, HepG2 cells were incubated with Lac-BSA-FND and dynasore, a cell-permeable inhibitor of dynamin, in the cell medium. The inhibitor is known to suppress lamellipodia formation by destabilizing actin filaments.[48,49] With the cells pretreated with 0.24 mM dynasore for 1 h, we observed a ≈10-fold decrease in fluorescence intensity (Figure 5b), which supports the suggestion that the cellular uptake of Lac-BSA-FND is contributed primarily by receptor-mediated endocytosis.

2.5. Antibody-Based Labeling

Two breast cancer cell lines, ASB145-1R and MCF-7, were used for a comparative study of antigen targeting. These two cell types have different CD44 expression levels, as confirmed by dye labeling and flow cytometric analysis. **Figure 6**a,c compare the results for cells labeled with biotinylated anti-CD44 and subsequently stained with DyLight488-SA. More than 98% of the ASB145-1R cells are CD44-positive, whereas it is only ≈43% for the MCF-7 cells. The

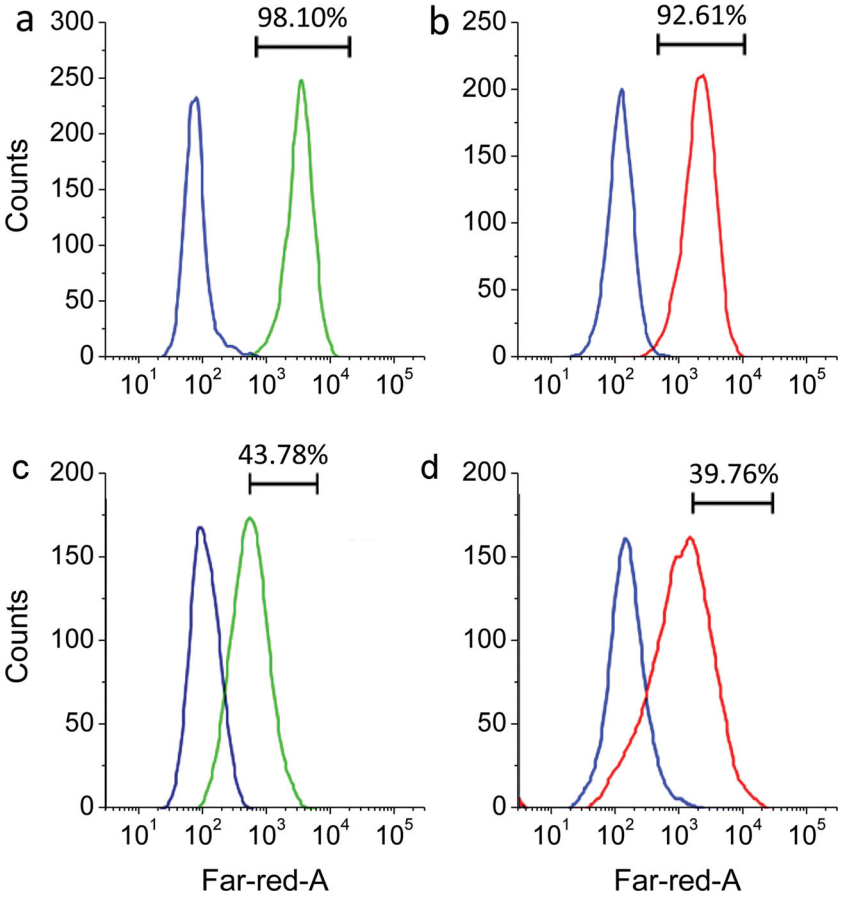

Figure 6. Flow cytometric analysis of the specific labeling of live CD44-expressed cells by DyLight488-SA and SA-PEG-FND. a,b) ASB145-1R cells and c,d) MCF-7 cells were labeled with DyLight488-SA (green) and SA-PEG-FND (red), respectively. Control experiments (blue) were performed following the same labeling procedures but without biotin-anti-CD44. Values above bars represent the percentages of CD44-positive cells.

marked difference in the CD44 expression levels allows easy separation of the cells by fluorescence-activated cell sorting (FACS) using the dye labeling.

Next, we applied the FND labeling technique to sort these two cell types by treating them with biotinylated anti-CD44 and then with SA-PEG-FND. However, in order to assess the level of CD44 expressed on the cell surface membrane using fluorescent nanoparticles as biolabels, both the ASB145-1R and MCF-7 cells have to be labeled at 4 °C to inhibit endocytosis. This limits the level of FND fluorescence, virtually precluding FACS analysis. Fortunately, using the higher-brightness FND, which has a fourfold increase in fluorescence intensity (Figure 1), enables discrimination of these two cell types with FACS. Shown in Figure 6b,d are the percentages of the CD44-positive cells determined by the FND labeling: 92.61% for ASB145-1R versus 39.76% for MCF-7 cells. The approximately twofold difference is in good agreement with that obtained by the DyLight488 staining. It is concluded from this result as well as the marked difference between the control and treatment groups that the labeling specificity of the SA-PEG-FND is high. Additionally, it indicates that the size of the nanoparticles is sufficiently small not to affect the interaction of biotin with the FND-labeled streptavidin.

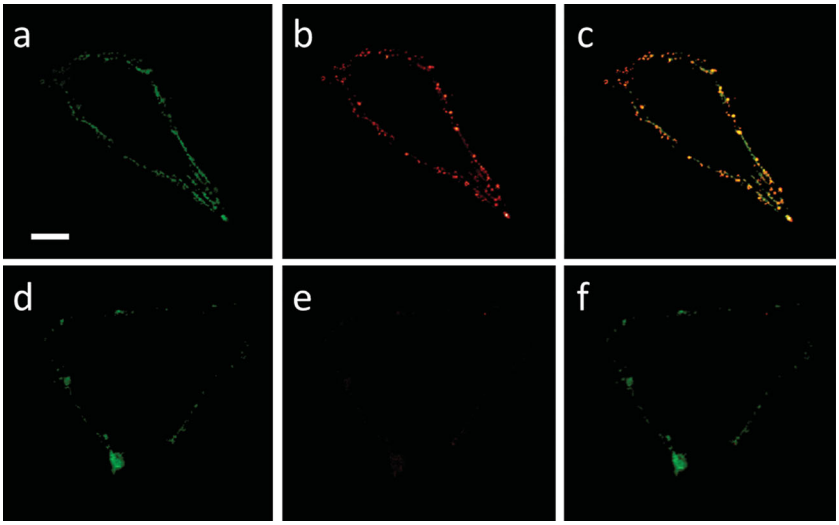

Figure 7. Colocalization studies of CD55-FND and HA-tag-Alexa-Fluor488 on the MDA-MB-231 cell surface over-expressing CD55-HA fusion proteins by confocal fluorescence microscopy. The cells were first labeled with anti-HA antibodies, and then incubated with anti-rabbit IgG conjugated with Alexa Fluor488 (green). Subsequently, cells were labeled a–c) with or d–f) without biotinylated anti-CD55 antibody, and then incubated with SA-PEG-FND (red). The corresponding merged images are shown in (c) and (f). Scale bar is 10 μm.

Another example to illustrate the high specificity of the FND labeling is the double staining of single membrane proteins. We chose to use a human breast cancer cell line, MDA-MB-231, which was infected to express a fusion protein, CD55-HA (i.e., CD55 conjugated with a HA tag), on cell membrane surface.[50,51] The fusion protein can be visualized concurrently by using both biotinylated anti-CD55 labeled with SA-PEG-FND and anti-HA labeled with AlexFluor488. As shown in **Figure 7** for confocal fluorescence images, the CD55-targeted FND colocalized almost completely with the HA-targeted Alexa Fluor488 on the cell surface (Figure 7a–c). In contrast, the CD55-HA expressing cells labeled by SA-PEG-FND in the absence of biotinylated anti-CD55 antibodies exhibited no FND fluorescence signals (Figure 7d–f).

Being photostable and biostable,[2,3] FND allows tracking of the fate of the targeted biomolecules in cells over an extended period of time.[7] As a proof of principle, we probed CD44 before and after endocytosis in ASB145-1R cells by the FND labeling technique. In this experiment, cells were first labeled with biotinylated anti-CD44 and then stained with either SA-PEG-FND for 2 h or DyLight488-SA for 30 min at 4 °C, after which cells were washed by PBS and incubated at 37 °C to facilitate endocytosis. **Figure 8**a–k display fluorescence images of the cells with dye- and FND-labeled CD44 on their surfaces before (panels a–h) and after (panels i–k) endocytosis. As shown, the dye labeling suffers from the problem of photobleaching, which prevented repeated examination and further studies of the endocytic pathway of CD44 by confocal fluorescence microscopy (panel d). In contrast, FND is non-photobleaching and resistant to degradation by enzymes or acids (panel h). They can be readily identified in endosomes/lysosomes through colocalization studies with the endo-lysosomal marker Rab7 (panels i–k).[52–54] The appearance of the yellow colocalization spots in the merged images indicates that the targeted FND particles follow the course of the endocytic pathway. The invariance in emission intensity of the internalized FND particles suggests that they can be used as photostable tracers for endosomes and lysosomes over long periods of time.[55]

3. Conclusions

Fluorescent nanodiamond is a new valuable tool for long-term labeling, imaging, tracking, and enrichment of cancer and stem cells. In this work, we have successfully used fluorescence-enhanced and protein-functionalized FND for targeted labeling of mammalian cells. Specifically, a facile noncovalent conjugation method is developed to functionalize FND with carbohydrate-bearing proteins for hepatic targeting. A different approach has also been developed for high-specificity labeling of cell surface antigens with biotinylated antibodies utilizing stretavidin-grafted FND. With further improvement of the fluorescence intensity and functionality of this carbon-based nanomaterial, it is expected that the bioconjugated FND will offer exciting new opportunities for a wide range of cell labeling and targeting applications.

4. Experimental Section

FND Production: Synthetic type Ib diamonds, Micron+MDA and RVD, were obtained from Element Six (USA) and Changsha Naiqiang

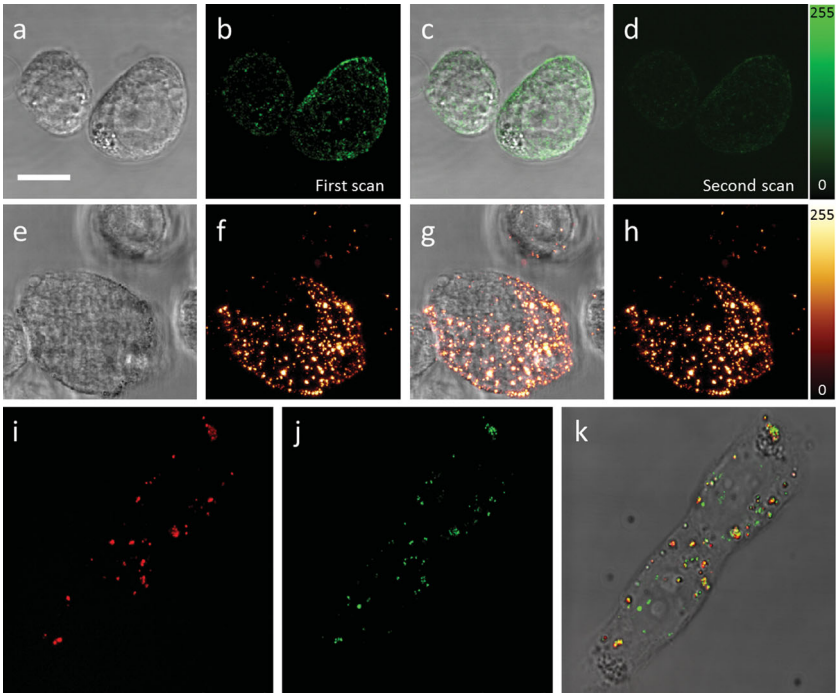

Figure 8. Bright-field and confocal fluorescence images of live ASB145-1R cells labeled with DyLight488-SA or SA-PEG-FND before and after endocytosis. The cells were first stained with biotinylated anti-CD44 antibody and then incubated with a–d) DyLight488-SA or e–h) SA-PEG-FND at 4 °C. Panels (a) and (e) are bright-field images, (b), (d), (f), and (h) are Z-stacked confocal fluorescence images, and (c) and (g) are merged bright-field and Z-stacked confocal fluorescence images of the cells before endocytosis. The contrast in photostability between these two types of fluorophores is evident in (d) and (h), where the organic dye is shown to be photobleached during the second scan of the specimen. i–k) FND-labeled CD44 on the cell surface was then internalized through endocytosis at 37 °C. The orange spots in the merged fluorescence image (k) evidence that the FND particles (red, i) are colocalized with endosome/lysosomes, which were stained by the endo-lysosomal marker, Rab7 (green, j). The nearly constant intensity of the FND fluorescence signal is an indication that the nanoprobes are non-photobleaching and resistant to degradation by enzymes or acids in endo/lysosomes. Scale bar is 10 μm.

Superabrasive (China), respectively. They were radiation-damaged by ion bombardment with either 3-MeV H^+ or 40-keV He^+ at a dose of ≈2 × 10^{16} H^+ cm^{-2} or ≈2 × 10^{13} He^+ cm^{-2}, respectively, followed by thermal annealing in vacuum at 800 °C for 2 h, surface oxidation in air at 490 °C for 2 h, and carboxylation in concentrated H_2SO_4-HNO_3 (3:1, v/v) at 100 °C for 3 h, as previously described.[26,27] The final size of the particles was determined by DLS using a particle size and zeta-potential analyzer (Delsa Nano C, Beckman-Coulter).

Noncovalent Conjugation of FND with (Neo)Glycoproteins: General procedures for the preparation of carbohydrate-modified BSAs have been described in Ref. [34]. In short, both Lac-BSA and TriGalNAc-BSA were prepared via reductive amination of the lysine residues of BSA (Sigma-Aldrich) using lactose and aldehyde-containing TriGalNAc, respectively. To conduct nanoparticle-protein conjugation, acid-treated FND (1 mg) was first thoroughly sonicated in DDW for 15 min and then mixed with BSA (5 nmol), Lac-BSA (5 nmol), TriGalNAc-BSA (10 nmol), or AF (10 nmol) by gentle shaking for at least 3 h at room temperature in DDW to allow physical adsorption. Afterwards, unbound proteins were removed by centrifugation (4 °C, 15 000 rpm, and 15 min) and the pellets were washed extensively with water and finally suspended in PBS. The dispersibility of FND in either DDW or PBS before and after the protein conjugation was examined by particle size measurement using DLS.

Covalent Conjugation of FND with Streptavidin: Acid-treated FND (1 mg) was thoroughly dispersed in acidic DDW (pH = 4) by sonication for 15 min. Next, *N*-(3-dimethylaminopropyl)-*N*′-ethylcarbodiimide hydrochloride (2 mg, EDC, Sigma-Aldrich) and *N*-hydroxysuccinimide (2 mg, NHS, Sigma-Aldrich) were added to the mixture to activate the surface carboxyl groups of FND for 30 min. After being separated by centrifugation and washed with basic DDW (pH = 8), the FND was PEGylated by mixing with *O*-(2-aminoethyl)-*O*′-(2-carboxyethyl) polyethylene hydrochloride (5 mg, molecular weight ≈ 3000, Sigma-Aldrich) for 6 h.[20] Afterwards, the PEG-FND was washed thoroughly by neutral DDW, and PEG-COOH was activated by EDC and NHS again to react with SA (200 μg, AnaSpec) for 5 h. Finally, the SA-PEG-conjugated FND particles were coated with BSA (1 mg) for 2 h to block residual open sites on surfaces. Size distributions of the FND bioconjugates before and after the reactions at each step were measured by DLS.

Cell Cultures: HepG2, a human liver carcinoma cell line, and MCF-7 and MDA-MB-231, both of which are human breast adenocarcinoma cell lines, were obtained from ATCC. ASB145-1R was a breast cancer cell line established in the lab of A. L. Yu at Genomics Research Center from cells expressing insulin-like growth factor 1 receptor (IGF-1R) sorted from a xenograft of primary breast cancer obtained from patient BC-145. HepG2 cells were cultured in Dulbecco's modified Eagle's medium (DMEM) containing 10% fetal bovine serum (FBS), 100 μg mL^{-1} penicillin, and 100 μg mL^{-1} streptomycin (Gibco-Invitrogen). MCF-7 and ASB145-1R cells were maintained in DMEM containing 10% FBS, 10 μg mL^{-1} bovine insulin (Sigma-Aldrich), 1.0 mM sodium pyruvate (Gibco-Invitrogen), 2 mM glutaMAX (Gibco-Invitrogen), 100 μg mL^{-1} penicillin, and 100 μg mL^{-1} streptomycin. MDA-MB-231 cells were cultured in high-glucose DMEM supplemented with 10% FBS, 2 mM glutaMAX, 100 μg mL^{-1} streptomycin, and 100 μg mL^{-1} penicillin. All the cell lines were grown at 37 °C and 5% CO_2 in a humidified air incubator with the culture periodically screened for mycoplasma infection.

Biotinylation of Anti-CD55: Anti-CD55 antibody (Santa Cruz Biotechnology) was biotinylated by mixing it with sulfo-NHS-biotin (Thermo Scientific) at a weight ratio of 4:1 in PBS at 4 °C for 2 h. The biotinylated anti-CD55 antibody was purified by a Pierce concentrator (20ml/9K MWCO, Thermo Scientific) at 4 °C.

CD55-HA Expressing Stable Cell Lines: DAF/CD55 genes with HA tags were subcloned into a mammalian expression vector (pSIN-EF2) carrying an EF1a promoter, an internal ribosome entry site (IRES), and a puromycin resistance gene.[56] The DAF/CD55 open-reading frame (ORF) fragment was prepared by PCR amplification of the gene from ATCC IMAGE Consortium Clone #3460621 with the addition of a SpeI site at the start of the coding region and an EcoRI sites at the end of the stop codon. The primers used for the amplification and HA tag insertion are as follows: forward primer, 5′-gcactagtgccgccgccatgaccgtcgcgcggccg-3′ (adds a SpeI site upstream of the ATG); reverse primer, 5′-gcgaattcctaagtcagcaagcccatgg-3′ (adds an EcoRI site downstream of the stop codon); HA tag insert forward primer, 5′-catacgatgttccagattacgctgactgtggccttcccccag-3′; and HA tag insert reserve primer, 5′-gtaatctggaacatcgtatgggtaaccccacacggccggcag-3′. To produce stable cell lines, cloned DNA was used for transfection with a retroviral packaging system into 293T cells. After 72 h of incubation, retrovirus-containing medium was collected, filtered (0.45 μm), and

applied to MDA-MB-231 cells with 8 μg mL^{-1} polybrene (Sigma-Aldrich). Cells were then selected in media containing 2 μg mL^{-1} puromycin (Sigma-Aldrich).

Hepatic Targeting: HepG2 cells were seeded at a density of 3×10^5 cells per 35-mm dish and cultured for 24 h. Cells were then incubated with 10, 25, and 50 μg mL^{-1} FND bioconjugates in serum-free DMEM at 37 °C and 5% CO_2 for 4 h, after which the FND-labeled cells were trypsinized and separated by centrifugation to remove free FND. They were then either resuspended in PBS for flow cytometric analysis or reseeded in culture plates for examination by confocal fluorescence microscopy.

Inhibition and Competition Assays: Inhibition assays were performed by pre-incubating 2×10^5 HepG2 cells with or without 0.24 mM dynasore (Sigma-Aldrich) for 1 h, followed by incubation with Lac-BSA-FND for 1–4 h at 37 °C. After washing away excess Lac-BSA-FND, the cellular uptake of Lac-BSA-FND was analyzed by flow cytometry after trypsinization. For the competition assay, 2×10^5 HepG2 cells were incubated with 50 μg mL^{-1} Lac-BSA-FND in the presence of 0.3 M lactose (Sigma-Aldrich) at 37 °C for 4 h. The cellular uptake was also analyzed by flow cytometry.

CD44 Targeting: ASB145-1R and MCF-7 cells were seeded separately at a density of 5×10^5 cells per 35-mm dish and cultured for 24 h. After trypsinization, cells were stained with biotinylated anti-CD44 antibody (0.5 μg, Biolegend) in PBS (100 μL) for 30 min and then treated with BSA blocking buffer in PBS (Bioshop) on ice for 30 min. Subsequently, the anti-CD44-stained cells were labeled with Dylight488-SA (0.5 μg, Thermo Scientific) in PBS (100 μL) on ice for 30 min or 250 μg mL^{-1} SA-PEG-FND in PBS on ice for 2 h. Excess labeling reagents were removed by PBS washes and centrifugation at 4 °C. Control experiments were performed following the same protocol except that the cells were not stained with biotinylated anti-CD44 antibody. Targeted cells were analyzed by flow cytometry and confocal fluorescence microscopy.

CD55-HA Targeting: MDA-MB-231 cells expressing CD55-HA were precultured in 35 mm dishes at a density of 3×10^5 cells per dish. Cells were then fixed by using 4% paraformaldehyde for 15 min and treated with 3% BSA blocking buffer for 30 min. Afterwards, cells were incubated with 0.2 μg mL^{-1} anti-HA antibody for 1 h and 2 μg mL^{-1} AlexFluor488 anti-rabbit antibody for 30 min. To conduct FND labeling, cells were first mixed with 4 μg mL^{-1} biotinylated anti-CD55 antibody for 1 h and then blocked with 3% BSA in PBS for 30 min. Cells were then labeled with 1 mg mL^{-1} SA-PEG-FND for 2 h in an inverted configuration (Supporting Information Figure S3), after which unbound SA-PEG-FND was removed by PBS washes. The specimens were finally sealed using Mowiol as the embedding medium.

Endo-Lysosomal Marking: ASB145-1R cells were fixed in 4% paraformaldehyde for 15 min and then treated with 0.5% Triton in PBS (1 mL) for 15 min to permeabilize cell membrane. After PBS washes, cells were incubated with 3% BSA in PBS for 30 min, followed by staining with anti-Rab 7 antibody (Rab7 (D95F2) XP Rabbit mAb, Cell Signaling Technology) for 40 min. Afterwards, cells were washed three times with PBS and subsequently were labeled with 2 μg mL^{-1} AlexaFluor488 or AlexaFluor594 anti-rabbit antibody for 30 min.

Fluorescence Spectroscopy: Fluorescence spectra of FND suspended in water (typically 1 mg mL^{-1}) were acquired with a home-built spectrometer as described previously.[26,27] It consisted of a 532-nm laser (DPGL-2100F; Photop Suwtech), a dichroic beam splitter (Z532RDC; Chroma Tech), a microscope objective lens (10×, NA 0.3, Nikon), a long-pass edge filter (E565LP; Chroma Tech), and a multichannel analyzer (C7473, Hamamatsu). Backward fluorescence from the sample was collected through the same objective to avoid strong light scattering loss and distortion of the fluorescence spectra.

Flow Cytometry and FACS: In hepatic targeting, the uptake of (neo)glycoprotein-modified FND by HepG2 cells were analyzed by a flow cytometer (FACSArray Bioanalyzer, BD Biosciences) equipped with a 532 nm laser. Typically 10,000 cells were examined in each measurement and the fluorescence signals of FND were detected at the emission wavelength of >590 nm. For antibody-based labeling, ASB145-1R and MCF-7 cells targeted with SA-PEG-FND were analyzed by using a cell sorting system (FACSAriaII, BD Biosciences). A 594 nm laser excited FND and the resultant fluorescence emission was collected through a 650 nm bandpass filter. A 488 nm laser and a 530/30 bandpass filter were additionally employed for the detection of DyLight488-labeled cells.

Confocal Fluorescence Microscopy: Confocal fluorescence images of cells were acquired by using an inverted microscope (SP5, Leica) equipped with two lasers operating separately at 561 nm and 488 nm for the excitation of FND and DyLight488, respectively. Fluorescence was collected through an oil-immersion objective (100×, NA 1.4) and detected with either a photomultiplier tube for DyLight488 or an avalanche photodiode for FND.

Supporting Information

Supporting Information is available from the Wiley Online Library or from the author.

Acknowledgements

B.-M.C. and H.-H.L contributed equally to this work. This work is supported by Academia Sinica and the National Science Council, Taiwan, with Grant No. 101-2628-M-001-005-. We thank V. Vaijayanthimala, Chiao-Yun Chien, and Chia-Ning Shen for discussion and assistance. We also acknowledge the excellent technical assistance, service, and advice provided by confocal cell imaging facility at the Division of Medical Biology, Genomics Research Center.

Received: March 28, 2013
Revised: May 9, 2013
Published online: July 22, 2013

[1] S. K. Nune, P. Gunda, P. K. Thallapally, Y.-Y. Lin, M. L. Forrest, C. J. Berkland, *Expert Opin. Drug Delivery* **2009**, *6*, 1175.
[2] V. Vaijayanthimala, P.-Y. Cheng, S.-H. Yeh, K.-K. Liu, C.-H. Hsiao, J.-I. Chao, H.-C. Chang, *Biomaterials* **2012**, *33*, 7794.
[3] S.-J. Yu, M.-W. Kang, H.-C. Chang, K.-M. Chen, Y.-C. Yu, *J. Am. Chem. Soc.* **2005**, *127*, 17604.
[4] C.-C. Fu, H.-Y. Lee, K. Chen, T.-S. Lim, H.-Y. Wu, P.-K. Lin, P.-K. Wei, P.-H. Tsao, H.-C. Chang, W. Fann, *Proc. Natl. Acad. Sci. USA* **2007**, *104*, 727.
[5] O. Faklaris, D. Garrot, V. Joshi, F. Druon, J.-P. Boudou, T. Sauvage, P. Georges, P. A. Curmi, F. Treussart, *Small* **2008**, *4*, 2236.
[6] K.-K. Liu, C.-C. Wang, C.-L. Cheng, J.-I. Chao, *Biomaterials* **2009**, *30*, 4249.
[7] C.-Y. Fang, V. Vaijayanthimala, C.-A. Cheng, S.-H. Yeh, C.-F. Chang, C.-L. Li, H.-C. Chang, *Small* **2011**, *7*, 3363.
[8] A. M. Schrand, J. Johnson, L. Dai, S. M. Hussain, J. J. Schlager, L. Zhu, Y. Hong, E. Osawa, in *Safety of Nanoparticles* (Ed: T. J. Webster), Springer, **2009**. *Ch.* 8.
[9] V. Vaijayanthimala, Y.-K. Tzeng, H.-C. Chang, C.-L. Li, *Nanotechnology* **2009**, *20*, 425103.
[10] N. Mohan, C.-S. Chen, H.-H. Hsieh, Y.-C. Wu, H.-C. Chang, *Nano Lett.* **2010**, *10*, 3692.
[11] R. J. McMahon, in *Avidin-Biotin Interactions*, Vol. *418*, (Ed: R. J. McMahon), Humana Press, **2008**.
[12] J. K. Jaiswal, E. R. Goldman, H. Mattoussi, S. M. Simon, *Nat. Methods* **2004**, *1*, 73.
[13] O. A. Shenderova, S. A. C. Hens, in *Nanodiamonds: Applications in Biology and Nanoscale Medicine* (Ed: D. Ho), Springer, **2010**, Ch. 4.
[14] W. S. Yeap, K. P. Loh, in *Nanodiamonds: Applications in Biology and Nanoscale Medicine* (Ed: D. Ho), Springer, **2010**, Ch. 5.

[15] H.-C. Chang, in *Nanodiamonds: Applications in Biology and Nanoscale Medicine* (Ed: D. Ho), Springer, **2010**, Ch. 6.
[16] H. J. Huang, E. Pierstorff, K. Liu, E. Osawa, D. Ho, in *Nanodiamonds: Applications in Biology and Nanoscale Medicine* (Ed: D. Ho), Springer, **2010**, Ch. 7.
[17] J.-I. Chao, E. Perevedentseva, C.-C. Chang, C.-Y. Cheng, K.-K. Liu, P.-H. Chung, J.-S. Tu, C.-D. Chu, S.-J. Cai, C.-L. Cheng, in *Nanodiamonds: Applications in Biology and Nanoscale Medicine* (Ed: D. Ho), Springer, **2010**, Ch. 9.
[18] A. Krueger, D. Lang, *Adv. Funct. Mater.* **2012**, *22*, 890.
[19] M. Mkandawire, A. Pohl, T. Gubarevich, V. Lapina, D. Appelhans, G. Rödel, W. Pompe, J. Schreiber, J. Opitz, *J. Biophotonics* **2009**, *2*, 596.
[20] B. Zhang, Y. Li, C.-Y. Fang, C.-C. Chang, C.-S. Chen, Y.-Y. Chen, H.-C. Chang, *Small* **2009**, *5*, 2716.
[21] M.-F. Weng, S.-Y. Chiang, N.-S. Wang, H. Niu, *Diamond Relat. Mater.* **2009**, *18*, 587.
[22] Y. Li, X. Zhou, *Diamond Relat. Mater.* **2010**, *19*, 1163.
[23] X. Q. Zhang, R. Lam, X. Y. Xu, E. K. Chow, H. J. Kim, D. Ho, *Adv. Mater.* **2011**, *23*, 4770.
[24] J. K. Lim, S. A. Majetich, R. D. Tilton, *Langmuir* **2009**, *25*, 13384.
[25] Y.-K. Tzeng, O. Faklaris, B.-M. Chang, Y. Kuo, J.-H. Hsu, H.-C. Chang, *Angew. Chem. Int. Ed.* **2011**, *50*, 2262.
[26] Y.-R. Chang, H.-Y. Lee, K. Chen, C.-C. Chang, D.-S. Tsai, C.-C. Fu, T.-S. Lim, Y.-K. Tzeng, C.-Y. Fang, C.-C. Han, H.-C. Chang, W. Fann, *Nat. Nanotechnol.* **2008**, *3*, 284.
[27] T.-L. Wee, Y.-W. Mau, C.-Y. Fang, H.-L. Hsu, C.-C. Han, H.-C. Chang, *Diamond Relat. Mater.* **2009**, *18*, 567.
[28] L.-J. Su, C.-Y. Fang, Y.-T. Chang, K.-M. Chen, Y.-C. Yu, J.-H. Hsu, H.-C. Chang, *Nanotechnology.* **2013**, *24*, 315702.
[29] C. Gabay, I. Kushner, *Acute-Phase Proteins*, John Wiley & Sons, **2001**.
[30] R. T. Lee, Y. C. Lee, *Glycoconjugate J.* **1987**, *4*, 317.
[31] P. K. Grewal, The Ashwell–Morell receptor, in *Methods in Enzymology*, (Ed: F. Minoru), Academic Press, **2010**, Ch. 13.
[32] Y. C. Lee, R. R. Townsend, M. R. Hardy, J. Lönngren, J. Arnarp, M. Haraldsson, H. Lönn, *J. Biol. Chem.* **1983**, *258*, 199.
[33] L. T. Braiterman, S. C. Chance, W. R. Porter, Y. C. Lee, R. R. Townsend, A. L. Hubbard, *J. Biol. Chem.* **1989**, *264*, 1682.
[34] Y. C. Lee, *Wiley Encycl. Chem. Biol.* **2009**, *3*, 298.
[35] R. T. Lee, M.-H. Wang, W.-J. Lin, Y. C. Lee, *Bioorg. Med. Chem.* **2011**, *19*, 2494.
[36] R. Kikkeri, B. Lepenies, A. Adibekian, P. Laurino, P. H. Seeberger, *J. Am. Chem. Soc.* **2009**, *131*, 2110.
[37] C.-H. Lai, C.-Y. Lin, H.-T. Wu, H.-S. Chan, Y.-J. Chuang, C.-T. Chen, C.-C. Lin, *Adv. Funct. Mater.* **2010**, *20*, 3948.
[38] M. Zöller, *Nature Rev. Cancer* **2011**, *11*, 254.
[39] J.-H. Mikesch, H. Buerger, R. Simon, B. Brandt, *Biochim. Biophys. Acta* **2006**, *1766*, 42.
[40] T. Takimoto, T. Chano, S. Shimizu, H. Okabe, M. Ito, M. Morita, T. Kimura, T. Inubushi, N. Komatsu, *Chem. Mater.* **2010**, *22*, 3462.
[41] X. Zhang, C. Fu, L. Feng, Y. Ji, L. Tao, Q. Huang, S. Li, Y. Wei, *Polymer* **2012**, *53*, 3178.
[42] X. L. Kong, L. C.-L. Huang, C.-M. Hsu, W.-H. Chen, C.-C. Han, H.-C. Chang, *Anal. Chem.* **2004**, *77*, 259.
[43] W.-H. Chen, S.-C. Lee, S. Sabu, H.-C. Fang, S.-C. Chung, C.-C. Han, H.-C. Chang, *Anal. Chem.* **2006**, *78*, 4228.
[44] T. K. Dam, H.-J. Gabius, S. André, H. Kaltner, M. Lensch, C. F. Brewer, *Biochem.* **2005**, *44*, 12564.
[45] T. T. B. Ngyuen, H.-C. Chang, V. W.-K. Wu, *Diamond Relat. Mater.* **2007**, *16*, 872.
[46] J. F. Hancock, *Nat. Rev. Mol. Cell Biol.* **2006**, *7*, 456.
[47] E. C. Cho, Q. Zhang, Y. Xia, *Nat. Nanotechnol.* **2011**, *6*, 385.
[48] E. Macia, M. Ehrlich, R. Massol, E. Boucrot, C. Brunner, T. Kirchhausen, *Dev. Cell* **2006**, *10*, 839.
[49] S. Poirier, G. Mayer, V. Poupon, P. S. McPherson, R. Desjardins, K. Ly, M.-C. Asselin, R. Day, F. J. Duclos, M. Witmer, R. Parker, A. Prat, N. G. Seidah, *J. Biol. Chem.* **2009**, *284*, 28856.
[50] R. J. Russell, P. S. Kerry, D. J. Stevens, D. A. Steinhauer, S. R. Martin, S. J. Gamblin, J. J. Skehel, *Proc. Natl. Acad. Sci. USA* **2008**, *105*, 17736.
[51] S. Yamada, Y. Suzuki, T. Suzuki, M. Q. Le, C. A. Nidom, Y. Sakai-Tagawa, Y. Muramoto, M. Ito, M. Kiso, T. Horimoto, K. Shinya, T. Sawada, M. Kiso, T. Usui, T. Murata, Y. Lin, A. Hay, L. F. Haire, D. J. Stevens, R. J. Russell, S. J. Gamblin, J. J. Skehel, Y. Kawaoka, *Nature* **2006**, *444*, 378.
[52] Y. Feng, B. Press, A. Wandinger-Ness, *J. Cell Biol.* **1995**, *131*, 1435.
[53] T. Wang, Z. Ming, W. Xiaochun, W. Hong, *Cell Signal* **2011**, *23*, 516.
[54] S. Meresse, G. Jean-Pierre, C. Philippe, *J. Cell. Sci.* **1995**, *108*, 3349.
[55] K. Hanaki, A. Momo, T. Oku, A. Komoto, S. Maenosono, Y. Yamaguchi, K. Yamamoto, *Biochem. Biophys. Res. Commun.* **2003**, *302*, 496.
[56] J. Yu, M. A. Vodyanik, K. Smuga-Otto, J. Antosiewicz-Bourget, J. L. Frane, S. Tian, J. Nie, G. A. Jonsdottir, V. Ruotti, R. Stewart, I. I. Slukvin, J. A. Thomson, *Science* **2007**, *318*, 1917.